Sensors and Actuators B 156 (2011) 840–848

Contents lists available at ScienceDirect

Sensors and Actuators B: Chemical

journal homepage: www.elsevier.com/locate/snb

Sensor array-based optical portable instrument for determination of pH

A. Martinez-Olmos[a], S. Capel-Cuevas[b], N. López-Ruiz[a], A.J. Palma[a], I. de Orbe[b], L.F. Capitán-Vallvey[b,*]

[a] Department of Electronics and Computer Technology, Campus Fuentenueva, Faculty of Sciences, University of Granada, E-18071 Granada, Spain
[b] Department of Analytical Chemistry, Campus Fuentenueva, Faculty of Sciences, University of Granada, E-18071 Granada, Spain

ARTICLE INFO

Article history:
Received 24 November 2010
Received in revised form 21 February 2011
Accepted 23 February 2011
Available online 3 March 2011

Keywords:
Full-range optical pH sensor array
OLED display
Digital colour detector
HSV colour space
Portable instrumentation

ABSTRACT

A portable optical instrument is presented that makes it possible to determine pH with a colorimetric sensor array. The use of four membranes containing acid–base indicators makes it possible to cover the full range of pH using the *H* (hue) coordinate measurements of the HSV colour space. pH sensitive membranes were directly cast onto a plastic support to form a two-dimensional array, located between an OLED display as the programmable light source and a set of digital colour detectors. The resulting microcontroller-based system is immune to optical and electrical interferences. A complete optical and electrical characterization and optimization of the hand-held instrument was carried out. The instrument was used to determine pH using a simple algorithm to select the sensor output that was programmed in the microcontroller. The initial eleven candidate pH membranes were reduced to only four, which permit to obtain reliable pH values. The pH response of the selected four sensing elements was modelled, and calibration curves were applied to a validation set and real samples obtaining positive correlations between the real and predicted data.

1. Introduction

Chemical imaging is an analytical technique that combines standard digital imaging techniques with a variety of spectroscopic techniques, typically based on absorption, transmission or scattering (Raman) or emission (fluorescence, chemiluminescence) to provide the spatial distribution of sample components. It is of general use in a variety of industries to characterize both chemical composition and morphology [1].

With sensors, chemical imaging must use a detector array to monitor the desired chemical species with a number of distributed selective chemical sensors providing spatial resolution as well [2]. One example is microarray technology, with which the simultaneous analysis of thousands of analytes is possible in a single experiment such as array-based gene expression analysis or protein microarrays based on antigen–antibody or ligand–receptor reactions [3].

Different macroarrays have been described for the simultaneous analysis of a small number of analytes by means of different types of imaging devices. Examples of positional or two-dimensional arrays include the device described for iron speciation and full-range pH determination by immobilizing reagents on cellulosic paper and RGB coordinates [4,5]; an electrochemiluminescent enzymatic biosensor screen-printed array for L-lactate and D-glucose [6]; an array of individually addressable sites on a micromachined silicon chip containing microspheres derivatized with dehydrogenases for the fluorescent determination of β-D-glucose and β-D-galactose [7] and fluorescent specific reagents for common ions in water arranged in microtiter plates and based on luminescence decay time imaging [8]. Some examples of encoded bead macroarrays can be found in the literature, such as an optical imaging fiber for pH, O_2 and CO_2 in solutions [9].

However, the disadvantages of these approaches based on specific receptors – difficulties in obtaining good selectivity against similar analytes and the number of sensors needed, which increases proportionally with the number of analytes – have led to an alternative paradigm based on general or differential receptors [10]. This concept results in arrays of non-specific or low selective sensors (electronic tongues/noses) that produce analytical signals useful for the analysis of multi-component samples that are later treated through advanced mathematical procedures for signal processing by pattern recognition and/or multivariate analysis both for qualitative and quantitative analysis [11]. Different experimental approaches have been proposed based on non-selective arrays and imaging, such as: arrays of optical fibers, with the sensing phase located on the distal extreme [12] or incorporated into microspheres situated in microcavities etched into the end of the fiber [13]; arrays of polymeric microspheres with chemically modified surfaces that enable the covalent binding of receptors (conventional reagents, enzymes, and antibodies) and arranged in

* Corresponding author.
E-mail address: lcapitan@ugr.es (L.F. Capitán-Vallvey).

0925-4005/$ – see front matter © 2011 Elsevier B.V. All rights reserved.
doi:10.1016/j.snb.2011.02.052

micromachined cavities in Si structures [14,15]; arrays of molecular printing polymers used to discriminate between aromatic amines based on absorbance variation and linear discriminant analysis [16]; arrangement of reagents in microplate wells imaged by means of a CCD camera based on quenching fluorescence [17]; and arrays of colorimetric membranes placed on hydrophobic silica base retrieving colour change using a scanner [18].

In this report, a disposable optical sensor array was used to determine pH in the full-range. pH in optical sensors is a function of the concentration of the acid and basic forms of the indicator [19]. Thus, calibration functions in pH sensors come from mass–action law relationships between the pH and the optical signal typically resulting in narrow sigmoid shape dependence according to the Henderson–Hasselbalch equation. The main drawbacks of optical pH sensors are a short dynamic working range (2–3 pH units) and non-linear response, which requires different sensing membranes to cover the whole pH range, although different strategies have been devised to extend the working range of optical pH sensors [20].

Previous work by our group was focused on the development of a disposable optical sensor array to predict the pH of a solution in the full-range (0–14). This pH determination was obtained from the hue (H) values of the HSV colour space using a scanner to image the optical array containing 11 sensing elements with immobilized pH indicators and using diverse mathematical modelling [20,21]. In the first case [20] three different approaches for pH prediction were studied: Linear model, Sigmoid competition model and Sigmoid surface model, providing mean square errors (MSE) of 0.111, 0.075 and 0.266, respectively, for tap and river water samples. Then, neural networks were used as a prediction technique [21]. The best network structure obtained with the traditional trial-and-error procedure using the Levenberg–Marquardt training algorithm was made up of 11 input neurons, 10 hidden neurons and one output neuron for pH prediction, providing an MSE of 0.043.

Here, a handheld instrument is presented for the measurement of pH using a disposable optical sensor array with a more simple electronics than our previously designed photometers [22,23]. The acquisition of colour information from the array is obtained with a wide and programmable light source and a set of colour detectors that output the measured RGB coordinates coming from each membrane, in digital format, and used to calculate the *H* of the HSV colour space as the analytical parameter. In this paper, a complete optical and electrical characterization of the instrument is carried out and its application for the determination of pH in the whole range is detailed.

2. Experimental

2.1. Reagents

The chemicals used to prepare the pH sensitive films were potassium tetrakis (4-chlorophenyl)borate (TCPB, CAS No. 14680-77-4), tridodecylmethylammonium chloride (TDMAC, CAS No. 7173-54-8), aliquat 336 (CAS No. 5137-55-3), o-nitrophenyloctylether (NPOE, CAS No. 37682-29-4), dioctyl sebacate (DOS, CAS No. 122-62-3), bis(1-butylpentyl)adipate (BBPA, CAS No. 77916-77-9), tributyl phosphate (TBP, CAS No. 126-73-8), high molecular weight polyvinyl chloride (PVC, CAS No. 9002-86-2), cellulose acetate (CA, CAS No. 9004-35-7), ethyleneglycol (EG, CAS No. 107-21-1) and tetrahydrofuran (THF, CAS No. 109-99-9) all purchased from Sigma (Sigma–Aldrich Química S.A., Madrid, Spain). Bromothymol blue (CAS No. 76-59-5), phenol red (CAS No. 143-74-8), thymol blue (CAS No. 76-61-9), m-cresol purple (CAS No. 2303-01-7) and PAN (CAS No. 85-85-8) from Sigma, liphophilized Nile blue (CAS No. 125829-24-5) and purpurin (CAS No. 81-54-9) from Fluka (Fluka, Madrid, Spain), cresol red (CAS No. 1733-12-6) from Panreac (Panreac, Barcelona, Spain), alizarine (CAS No. 72-48-0) from TCI (TCI Europe, Belgium), and sicomet red P (CAS No. 5281-04-9) from BASF (BASF, Ludwigshafen, Germany) were used as acid–base indicators. As support sheets, Mylar-type polyester (Goodfellow, Cambridge, UK) was used. HCl and NaOH were supplied by Sigma. All reagents were of analytical reagent grade and were used without any further purification. All aqueous solutions were prepared in reverse-osmosis type quality water (Milli-RO 12 plus Milli-Q station from Millipore, conductivity 18.2 mS).

2.2. Instrumentation and software

The optical spectra were measured with a mini-spectrometer RC series C11007MA (Hamamatsu Photonics, Japan) with 256 pixels, spectral resolution at 9 nm half width and 16 bits of intensity resolution. For the electrical characterization of the prototype, the following instrumentation was used: a mixed signal oscilloscope (MSO4101, Tektronix, USA), a 6½ digit multimeter (34410A, Agilent Technologies, USA), a 15 MHz waveform generator (33120A, Agilent Technologies, USA) and a DC power supply (E3630A, Agilent Technologies, USA). For the image acquisitions and digitalization, a commercial scanner ScanMaker i900 (Microtek, Taiwan) was used, with a 6400 × 3200 dpi resolution, a maximum optical density of 4.2 and 24–48 bits of colour. The software to manage the scanner was Silver Fast Ai provided by Microteck. The images were processed with a set of scripts and functions developed by us in Matlab r2007b (The MathWorks, Inc., Natick, MA, USA). Statistical calculations were performed with the Statgraphics software package (Manugistics Inc. and Statistical Graphics Corporation, USA, 1992), and Microsoft Excel (Microsoft Corp., Redmond, WA, USA) was used for general calculations. A Crison pH-meter (Crison Instruments, Barcelona, Spain, model Basic 20) with a combined double junction glass electrode, calibrated against two standard buffer solutions (pH 4.0 and 7.0), was used for the pH measurements.

2.3. Sensor array preparation

The sensor array was prepared on a 5 cm × 4 cm transparent Mylar polyester support covered with an adhesive black film of PVC with 12 holes (3 columns and 4 rows), 5 mm diameter each. A black opaque film was used to reduce the light dispersion and prevent cross information between the sensing elements (Fig. 1). The sensing films were cast by carefully placing 8 μL of the corresponding cocktail in each hole, whose surface tension and quick evaporation make it possible to prepare the sensing membrane. The different cocktails for the pH membranes were prepared by dissolving the different chemicals needed in 1 mL of distilled THF according to the composition indicated in Table 1.

The pH sensor arrays were prepared according to the conditions of: (a) no leaching; (b) a tonal colour coordinate change from the reaction; and (c) full coverage of the pH range by overlapping the responses of the different membranes. The selected sensing elements were prepared from different cocktails containing different types and amounts of colorimetric acid–base indicators, polymers, plasticizers, lipophilic salts and, if necessary, humectant.

The composition of the different sensing elements was optimized considering leaching minimization (lipophilic salt, plasticizer, and membrane polymer), colour intensity (acid–base indicator) and response time (plasticizer, membrane polymer, humectant and cocktail volume). As a result, 11 different membranes, containing 10 different pH indicators, were prepared to cover the whole pH range.

Two different sensor arrays were prepared, both with the same structure. The first array contained the 11 different sensing elements studied and the second, the 4 pH membranes selected as

Table 1
Composition of the membranes (% w/w) used for the pH sensor array selection.

Membrane	Indicator (%)	Lipophilic salt (%)	Plasticizer (%)	Membrane polymer (%)	Humectant (%)
S1	Sicomet red P (1.41)	Aliquat 336 (5.63)	NPOE (66.20)	PVC (26.76)	–
S2	m-Cresol purple (3.00)	TDMAC (13.47)	DOS (28.00)	CA (33.00)	EG (22.57)
S3	PAN (1.43)	TDMAC (10.00)	NPOE (65.00)	PVC (23.60)	–
S5	Purpurin (1.43)	TDMAC (8.29)	NPOE (67.00)	PVC (23.29)	–
S6	Cresol red (1.43)	Aliquat 336 (4.54)	NPOE (67.00)	PVC (27.00)	–
S7	Liphophilized Nile blue (1.43)	TCPB (3.63)	TBP (67.00)	PVC (27.91)	–
S8	Bromothymol blue (3.00)	TDMAC (4.00)	DOS (28.00)	CA (37.00)	EG (19.60)
S9	Alizarin (1.43)	TDMAC (10.29)	NPOE (67.00)	PVC (21.3)	–
S10	Thymol blue (3.14)	TDMAC (11.57)	DOS (28.00)	CA (37.00)	EG (20.43)
S11	Phenol red (1.43)	TDMAC (6.93)	BBPA (26.00)	CA (30.00)	EG (35.64)
S12	Thymol blue (5.00)	TDMAC (18.40)	DOS (28.00)	CA (33.00)	EG (15.60)

the pH sensor array, with three replicates each. Additionally, one empty position of the support (S4) was used to test the illuminant of the instrument.

2.4. Description of the instrument

The block diagram of the portable instrument developed is presented in Fig. 2. This is a microcontroller-based system designed to measure the colour of an array of colorimetric sensing elements using their illumination with a programmable light source and collecting their transmitted light in an array of digital colour detectors. In this case, the measurement platform was used to measure the pH of a solution.

The microcontroller in this prototype was model PIC18F4550 (Microchip Technology Inc., USA) which was selected because of the integration of a USB module that allows easy communication with the computer for design and calibration purposes, and the availability of five input–output ports to control all the other modules. The user interface of the portable instrument consists of a small keypad which lets the user select different measurement options through a menu which is presented on the LCD screen. The results of the measurements are also visible on this screen, although they can be also stored in an EEPROM memory for further processing.

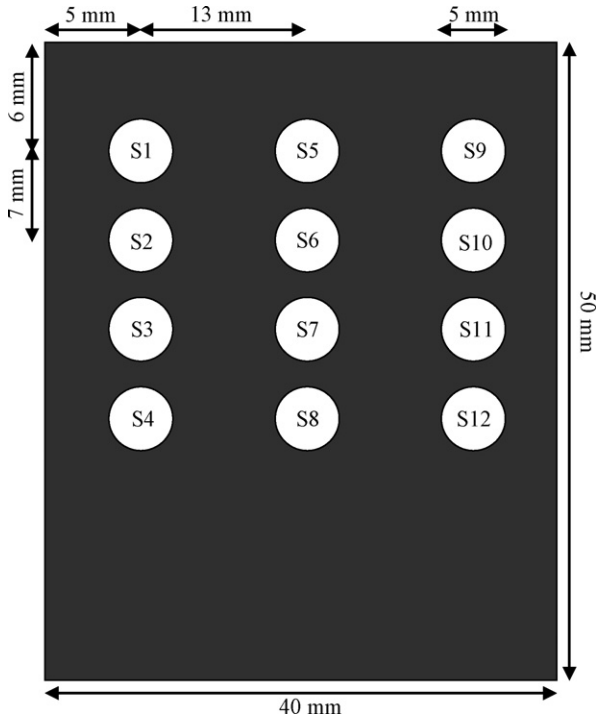

Fig. 1. Design of the sensor array support indicating membrane positions and dimensions.

2.4.1. Colour measuring module

This module is made up of an organic light-emitting diode display (OLED) working as a programmable light source [24,25] and twelve S9706 digital colour detectors (Hamamatsu Photonics, Japan) aligned with the sensor array. The light source is implemented by an OLED display, model 160-GMD1 (4D Systems, Australia), which communicates with the microcontroller via a two-wire serial bus. This is a compact, cost effective, all-in-one OLED display with an embedded graphics controller. The advantages of using this programmable light source against a light emitted diode (LED) lie on the possibility of the correction of the alignment with the detectors and the configuration of the light source by software. Due to these reasons the OLED was selected as light source despite its lower irradiance. The embedded commands not only control the background colour, but can produce text in a variety of sizes as well as draw shapes in 65 K colours while freeing up the host processor from screen control functions. Some of its main features are: 160×128 pixel resolution, 1.69″ diagonal with an active area of 33.6×26.9 mm, only 5 pin interface to any host device, voltage supply from 3.6 V to 6.0 V and 40 mA nominal current when using a 5.0 V supply source, serial RS-232 (0–3.3 V), onboard micro-SD (μSD) memory card adaptor for storing illumination patterns and built-in graphics commands.

The colour measurement of the transmitted light through the sensor array is carried out with a set of 12 (3×4) colour detectors, model S9706 (Hamamatsu Photonics, Japan). This device is a digital colour sensor sensitive to red, green and blue spectral regions, which makes the simultaneous measurement of RGB colour coordinates possible. The chip integrates a set of photodiodes whose maximum sensitivity wavelength corresponds to the previous colours ($\lambda_r = 615$ nm, $\lambda_g = 540$ nm and $\lambda_b = 465$ nm). The induced current of these photodiodes is on-chip processed to generate a digital output. This can be used to identify the colour of each element of the sensor array. The detected signals are serially output as 36-bit words, which make it possible to connect the sensors to the microcontroller without any need for additional signal processing. To enable measurement over a wide range of illuminants, the S9706 detector has two configuration parameters to select its active area and integration time. Internally, the active area of each detector (with dimensions of 1.2×1.2 mm) consists of 9×9 silicon photodiode elements in a mosaic, alternating red, blue and green sensitivity, and can be configured in a high sensitivity mode, where the full area collects the incident light, or in a low sensitivity mode, where a 3×3 centre area is chosen to be active. In this work, a high sensitivity mode was always chosen to cover the entire membrane surface. The output of each detector was connected to a different input pin of the microcontroller. With this configuration, the measurement of all the membranes could

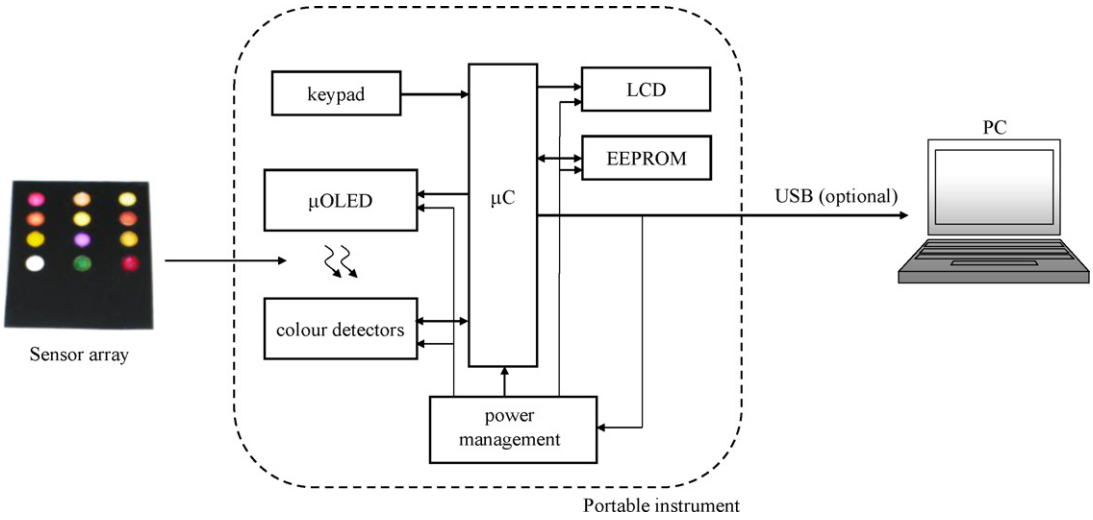

Fig. 2. Block diagram of the developed instrument.

be carried out at the same time, providing a fast response from the instrument.

2.5. Measurement procedure

The colour determination of the pH membranes was performed by measuring the transmitted light as follows: the sensor array was placed in the path of the light source from the programmable OLED display to the colour detector. In this design, the structure formed by the display and the colour detectors was shielded to prevent interferences due to external light; therefore, the instrument was enclosed in a black box with only one small opening to insert the sensor array board.

After the sensor array board was inserted into the instrument, the illumination pattern from the OLED display consists of a black background with the sequential illumination of circles (3×4), each aligned with an element of the sensor array and the corresponding colour detector. The pattern is not a static image, but a graphic sequence where the light source (circle) for each sensing element position only appears during the measurement of this element. Therefore, the illumination of each sensing element is done individually instead of simultaneously, in order to prevent stray light interference. The centre and the radii of these circles can be configured using software, which makes it possible to easily correct the alignment with the colour detectors. The photo in Fig. 3 shows the arrangement of the colour detectors and the light source pattern.

The response of the measurement system was evaluated for each 0.1–0.2 pH unit from 0 to 14 by adding volumes of 1.0 M, 0.1 M or 0.01 M of HCl or of NaOH with a microburette to an aqueous solution containing the sensor array hanging from a support with a clamp. After each addition and magnetic stirring, the pH of the solution was measured using a potentiometric procedure. The array sensor was equilibrated for 5 min, and then was pulled out and inserted into the instrument to be measured.

3. Results and discussion

This section first discusses the results of the characterization and optimization of the measurement system, indicating the optimal configuration of the programmable light source, digital colour sensors and measurement conditions of the complete instrument. Later, a detailed discussion of its use as a pH-meter will be carried out, including a comparison with a laboratory colorimetric system, a study of the minimum number of sensing elements for univocal and precise determination of the pH with complete instrument modelling and calibration. Finally, this calibration of the system will be validated and applied to real samples.

3.1. Characterization and optimization of measurement setup

3.1.1. OLED display

It is an advisable practice in colorimetric applications to use a light source as one of the standard illuminants. One of the most used illuminants is sunlight, such as the D65 illuminant [26]. As mentioned before, the light source used in the instrument is an OLED display which makes it possible to define up to 65,536 colours using the combination of three codes from 0 to 31 for the red and blue, and from 0 to 63 for green colour organic LEDs, all of which form the display. If the combination (31, 63, 31) is programmed in the display, its "white" colour is obtained. In Fig. 4, the spectrum of this white colour is displayed showing a notable excess of the blue component produced by the internal display configuration. Additionally, this figure shows the three separated spectral components, i.e., the (31, 0, 0), (0, 63, 0) and (0, 0, 31) colour codes corresponding to the separate activation of the red, green and blue organic LED of the display, respectively. Since the white colour has an excessive blue component – and in order to obtain an illuminant closest to

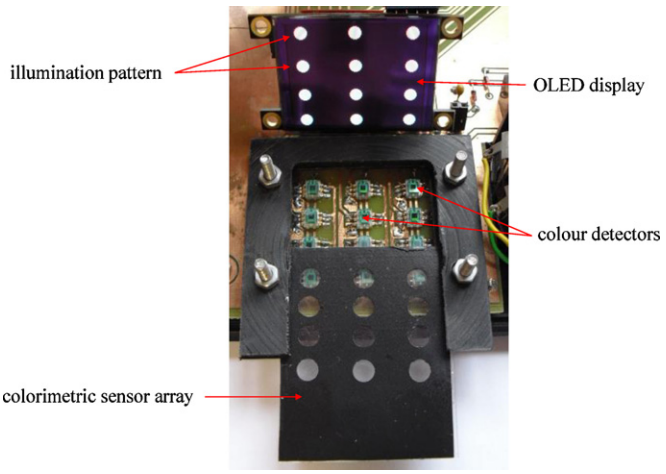

Fig. 3. Photography of the sensing module showing the OLED display (with illumination circles), the colorimetric sensor array support and the digital colour detector array.

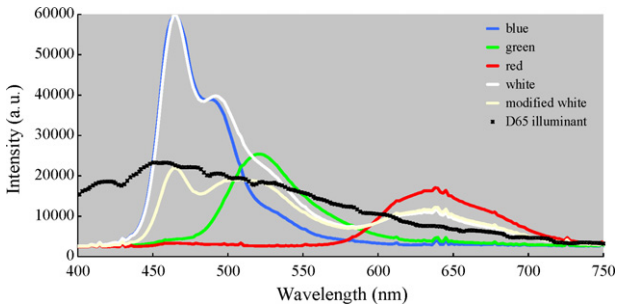

Fig. 4. Spectra of the OLED display and D65 standard illuminant.

the D65 standard – it was necessary to try other component combinations. The best result of this optimization process, reducing the blue component contribution, is shown in Fig. 4 and called "modified white", where the D65 spectrum is also shown with symbols for comparison. All the illuminant spectra depicted in Fig. 4 were tested as possible light source configurations. Best results were obtained with the "modified white"; therefore it was used as light source for the colour measurements. Given the spectral responses of the three RGB components of the display, some differences with the D65 spectrum can be observed, mainly below 450 nm and in the 525 to 600 nm spectral regions. Of course, these illuminant deficits will induce lower transmittance levels compared with those systems which have an illuminant closer to the D65 illuminant. Therefore, a priori, some differences may appear between this instrument and others.

In addition to the colour selection, the light intensity can be configured in this display. There are 16 levels of intensity from 0 (total darkness) to 15 (maximum brightness). The influence of this parameter was also analyzed, showing that an intermediate intensity range from 5 to 8 provides the best results for the sensing element array, showing a relative standard deviation (RSD) in the measured *H* value of 2.5%.

After configuring an adequate illuminant spectrum and intensity, the lighting uniformity of the display was analyzed by sensing the emitted light with the digital colour sensor placed facing it in different positions. The results showed that the output signal presents no variation when the sensor is moved within the display area. Moreover, the stability of the display, as well as the velocity of the response, was tested measuring the light emitted when the display was switched on and off in alternate cycles from the modified white to black, as shown in Fig. 5. From this figure, it can be deduced that the light emission when the display is switched on is fast enough to prevent the need for time delays between the illumination and the measuring process. Moreover, Fig. 5 shows that the measured light is very stable and repetitive, with an RSD of 0.6% in *H* measurements.

As mentioned above, the light source for each sensing element is a circle with the modified white over a black background. The

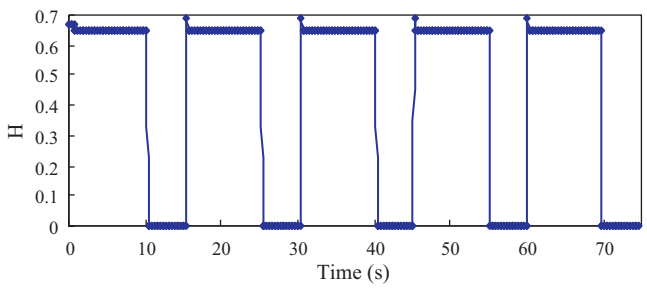

Fig. 5. Stability and velocity test for illumination of the display with the modified white colour.

influence of the circle diameter on the system performance was also studied. It has been demonstrated that this does not produce any significant variation in the coordinate *H* calculation (less than 5% RSD) in the diameter range from 5.75 to 10.25 mm taking into account a sensor element diameter of 5 mm. Despite this, the error source does not affect the system because the circle diameter was fixed at 6.35 mm in this study.

3.1.2. Digital colour detectors

In addition to the sensitivity modes related to the selected active area, this sensor can externally configure the integration time, i.e., the time interval during the photodiode matrix generates a photocurrent for each optical radiation acquisition. This integration time can be easily changed from 10 μs to 100 s with a unique input pin. According to the device datasheet, under constant illumination conditions, the sensor output increases linearly with this time until reaching output saturation. A short integration time means fast acquisition, but with low intensity light collection, i.e., low sensitivity, whereas with a longer integration time, the sensitivity increases, but with a slower acquisition and the possibility of sensor output saturation. Therefore, there is a compromise in the choice of this configuration parameter. We checked the response of this sensor as a function of the integration time in the typical illumination conditions for this application and concluded that the shortest time with optimal sensitivity and velocity of response was 200 ms. Moreover, our results show that there is no change in the *H* coordinate in the range from 150 ms to 500 ms, where the measured value presents an RSD of less than 0.8%.

Finally, the time stability of the S9706 detector response (integration time of 200 ms) was checked under continuous illumination. To reduce possible light source drifts, a white LED (NSPW300, Nichia, Japan), biased with a thermal stabilized current source, was used in this test, resulting in an output signal drift lower than 0.1%, acquiring a signal every 0.2 s during 90 min.

3.2. pH measurement

This section describes the procedure followed for the pH determination based on the colour measurements. First, the response of each sensing element in the full pH range was measured with the instrument. From these data, a minimization of the number of membranes needed for pH determination was carried out, reducing the initial array containing eleven elements to a four membrane array that covers the full pH range.

3.2.1. Characterization and minimization of the sensor array

The characterization of the sensor array was performed by measuring the *H* coordinate in the whole pH range using 12 replicate arrays. This was done by adding acid or base solutions to an aqueous solution containing the sensor array hanging from a support. As could be expected, the experimental curves for each membrane (Fig. 6) show the usual sigmoid shape, which in some cases was double.

The immobilized acid–base indicators belong to neutral, cationic and anionic types, and the heterogeneous reaction with acid or base in the membrane phase involves either ion-exchange or co-extraction mechanisms characterized by an equilibrium constant K_e which includes the acidity constant, the distribution constant between aqueous and membrane phases of different species, and the dissociation constants for the different ion-pairs involved. Table 2 shows the corresponding K_e calculated for each membrane along with the transition pH range, the colour and the *H* values for the acid and basic forms. Comparing the K_e values obtained with the portable instrument and those provided by a scanner working in transmission mode, some differences can be observed, although for purpurin, bromothymol blue and phenol red, the differences

Table 2
K_e values for sensing elements calculated from scanner and portable instrument H values.

Membrane	Indicator	pH range	Scanner	Portable instrument	Membrane colours	
			K_e	K_e	Acid	Base
S1	Sicomet red P	5.18–6.60	7.1×10^{-5}	2.7×10^{-5}	Nadeshiko pink (0.976)	Navajo white (0.089)
S2	m-Cresol purple	0–1.90	4.9×10^{0}	1.4×10^{0}	Wild watermelon (0.992)	Canary yellow (0.150)
		8.65–10.77	2.8×10^{-9}	3.2×10^{-9}	Mustard (0.128)	Persian indigo (0.881)
S3	PAN	7.57–10.95	3.4×10^{-9}	4.3×10^{-9}	Lemon (0.159)	Scarlet (0.023)
S5	Purpurin	1.90–4.56	2.0×10^{-3}	7.0×10^{-3}	Chrome yellow (0.110)	Carnation pink (0.960)
		12.44–13.81	9.4×10^{-7}	2.9×10^{-8}	Mauvelous (0.970)	Pastel magenta (0.945)
		–	7.3×10^{-10}	–	–	–
S6	Cresol red	7.35–3.19	4.3×10^{-9}	4.5×10^{-9}	Canary yellow (0.167)	Violet (0.644)
S7	Liphophilized Nile blue	9.46–11.99	1.3×10^{-10}	3.2×10^{-10}	Deep sky blue (0.520)	Cerise pink (0.917)
S8	Bromothymol blue	2.82–7.15	7.1×10^{-6}	2.5×10^{-4}	Pear (0.185)	Cadet blue (0.541)
S9	Alizarin	4.56–6.35	2.2×10^{-5}	2.0×10^{-4}	Maize (0.290)	Dark pastel blue (0.580)
S10	Thymol blue	0–0.85	3.7×10^{0}	5.5×10^{0}	Hot magenta (0.875)	Lemon (0.182)
		8.87–10.36	1.3×10^{-8}	4.4×10^{-9}	Yellow (0.207)	Celestial blue (0.582)
S11	Phenol red	5.37–6.80	1.2×10^{-8}	4.4×10^{-6}	Old gold (0.137)	Amaranth (0.963)
		9.46–11.40		3.3×10^{-10}	French rose (0.953)	Deep pink (0.905)
S12	Thymol blue	0–1.42	1.5×10^{0}	1.8×10^{0}	Deep cerise (0.979)	Golden yellow (0.127)
		9.04–11.56	3.7×10^{-9}	8.2×10^{-10}	Canary yellow (0.150)	Blue gray (0.609)

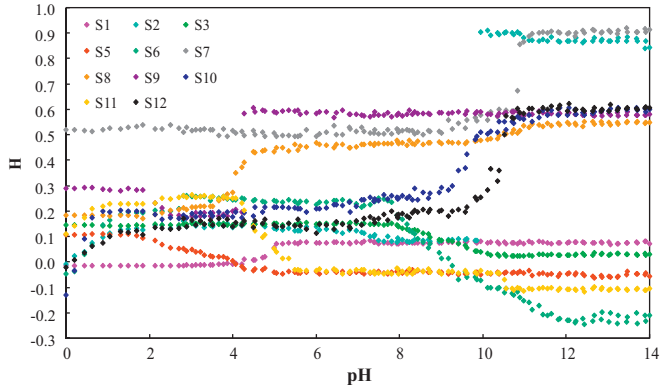

Fig. 6. Sensor array response (in H coordinates) to pH. Sensing element numbering was defined in Fig. 1.

were higher than one order of magnitude. The differences can be justified by differences in the illuminant and photodetectors used in each case.

As an example, Fig. 7 presents the responses obtained for two membranes (S2 and S12) with the new prototype and a commercial scanner. The response curves are very similar, although they were obtained in very different ways: while the line was generated from digital images acquired with the scanner and processed in the computer to calculate the corresponding H value [27], the symbols were obtained from the output data of the S9706 colour detectors, with no further processing. This implies a considerable reduction in the complexity of the determination of the pH. Similar results were obtained in the comparison with the rest of the sensing elements, showing only some minor discrepancies due to illuminant and detector differences.

From the response curves (Fig. 6), it can be seen that the colour changes of the sensor array membranes cover the full pH range. Table 2 presents the pH ranges where the different membranes exhibit some colour variation. As can be seen, there are many membranes whose response covers the same pH range, which makes it possible to reduce the number of elements due to the fact that they generate redundant information. Taking into account the data from Fig. 6 and Table 2, a minimization of the required membranes for full-range pH determination was done. The criteria followed for this minimization was selecting membranes with: (i) maximum H variation combined with maximum covered pH range and, (ii) minimum pH range overlapping. As a result, the sensing elements selected in this work were positions S2 (m-cresol purple membrane), S5 (purpurin membrane), S6 (cresol red membrane) and S8 (bromothymol blue membrane). The next section shows how to calculate a unique value of pH from the results of the colour measurements from only four sensing elements.

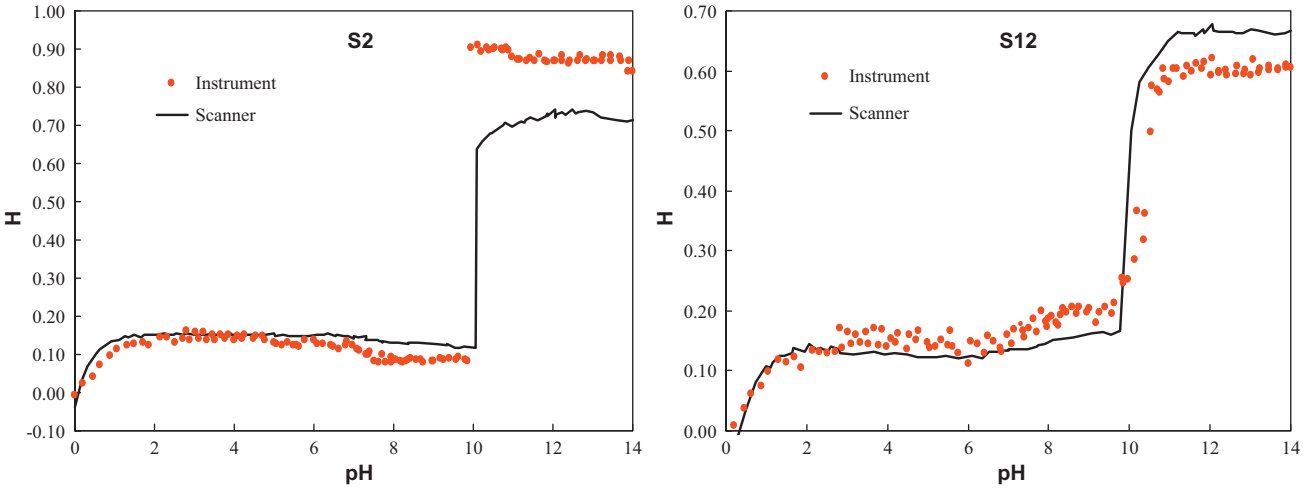

Fig. 7. Comparison of the pH response of S2 (left) and S12 (right) sensing elements measured with the proposed system (symbols) and the commercial scanner (lines).

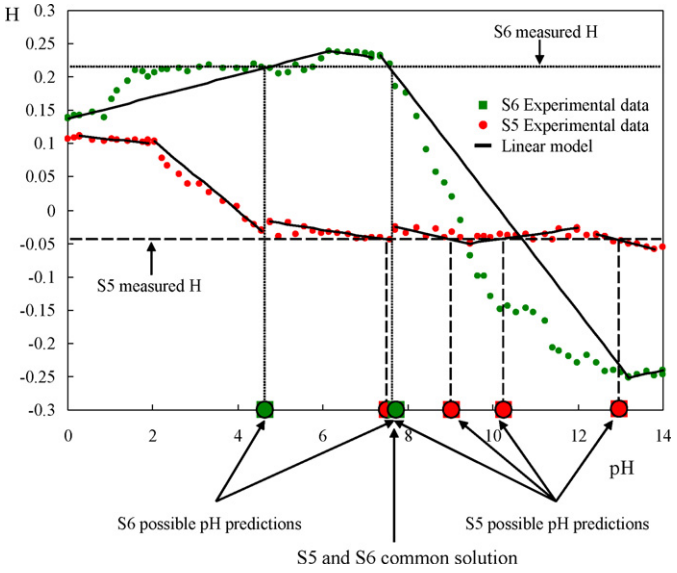

Fig. 8. Linear modelling of the membrane S5 and S6 responses (linear sections). Dashed horizontal lines represent measured *H* values with possible pH ranges for each sensing element and common pH range on the abscise axis.

3.2.2. Response modelling and pH calculation

Fig. 6 shows that the *H* value obtained for each sensing element can result in several values of pH in the full range, with only one of them being correct. Therefore, there is no univocal relationship between an *H* and a pH value with the selected four sensing elements if they are individually analyzed. To solve this, a two-step procedure is proposed. First, the pH range which includes the correct value must be determined. To do this, all the possible pH values of the sensing elements corresponding to the measured *H* coordinates need to be calculated. With this objective, the responses of the selected membranes were modelled, splitting them into increasing or decreasing linear sections, as depicted in Fig. 8 for membranes S5 and S6.

This figure presents an example of the possible pH predictions for a given *H* measurement. As can be seen, there are several points of pH that provide the same value of *H* for each membrane. The microcontroller solves each linear equation resulting from the linear section applied to the experimental *H* and generates a list of possible pH predictions. In the example in Fig. 8, these ranges correspond to Sections 2–5 in membrane S5, and Sections 1 and 3 in membrane S6. In this case, the only coincidence is found in Section 3 of each sensing element, indicating the approximate range where the final pH value will be. This process was repeated for the four selected membranes, obtaining four lists from which it is possible to determine the only range common to the four membranes as the correct solution. Since the linear model is not accurate, the pH ranges with the functioning corresponding sections are used as possible solutions, instead of the final pH values.

After this range was determined according to this method, a more precise pH value was calculated using a more accurate model of the corresponding sensing element response. Having to choose between the curve fit and the complex calculations needed for microcontroller programming, cubic polynomial modelling functions were selected. This made it possible to adjust the experimental data with high fidelity in the range of interest, i.e., the pH range where each sensing element changes its colour. These equations are simple enough to be able to calculate the pH with the microcontroller, which must provide a prediction of the pH within a short time after the colour measurements. Fig. 9 shows the experimental *H* values measured for the selected four sensors presented as symbols and the polynomial fit of these curves in the appropriate pH range, shown as lines. Thus, the fine modelling is done with these functions:

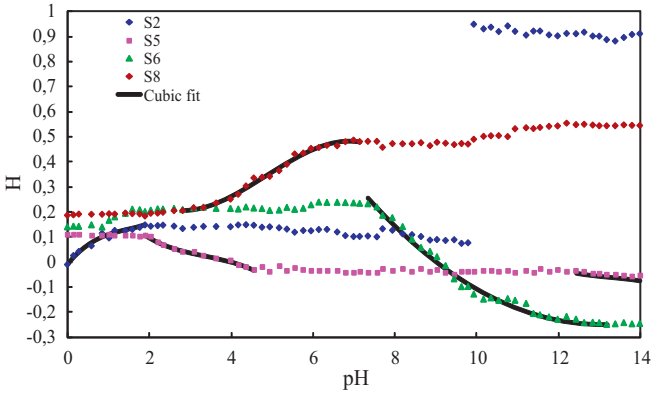

Fig. 9. Experimental *H* values of the four selected sensing elements (symbols) and cubic modelling (solid lines) for the pH ranges of interest.

$$H(\mathrm{pH}) = A + B \cdot \mathrm{pH} + C \cdot \mathrm{pH}^2 + D \cdot \mathrm{pH}^3 \quad (1)$$

The coefficients of the fit functions, as well as the pH range where they are defined, are listed in Table 3. It is must be noted that sensing element S5 was modelled in two different pH ranges. Finally, the pH calculation corresponding to a measured value of *H* was obtained by solving the third degree equation for the particular membrane modelled in the selected range.

This reconstruction algorithm was applied to a set of 102 validation data, with twelve replicates, covering the full pH range. We applied a Kolmogorov–Smirnov test to check whether the validation data set and the model prediction may be assumed to be normal. The confidence level of the test was the standard 80%, providing the probability values of 0.476 (validation set) and 0.259 (prediction for the validation set). Therefore, all the data distributions passed the test since the *p*-values were higher than 0.2. In order to test the prediction performance of the method, we applied a Student's *t*-test with a confidence level of 95%, to check whether the data distributions resulting from the predicted values in the validation data set differ significantly from the real data (using a potentiometric method as reference). The probability value obtained was 0.6593 (higher than 0.05), so we may conclude that the model is able to predict pH suitably since there are no significant differences between the real and predicted pH data. To finish the analysis, we applied a Pearson's correlation test to measure the quality of the predicted versus the real values. The result of the test provided a probability value under 2.2×10^{-16} in the validation data set, and we therefore may conclude that there is a significant correlation between the real and predicted values. Fig. 10A contains the regression line between the real and predicted data validation. The correlation coefficient R^2 was calculated and the test provided the value 0.997. Consequently, it may be assumed that the prediction model provides a suitable performance for the task of pH prediction. As can be seen, the pH predictions fit the original pH values with high fidelity in the range from 0 to 14, although the accuracy decreases for pH values higher than 13, due to the lower

Table 3
Cubic modelling coefficients, indicating valid pH ranges.

Membrane	*A*	*B*	*C*	*D*	R^2	pH range
S2	−0.006	0.200	−0.109	0.024	0.973	0–1.90
S5	0.566	−0.416	0.113	−0.011	0.991	1.90–4.56
S8	0.794	−0.483	0.121	−0.008	0.991	2.82–7.15
S6	2.582	−0.459	0.020	−0.0002	0.988	7.35–13.19
S5	17.047	−3.840	0.288	−0.007	0.966	12.44–14.0

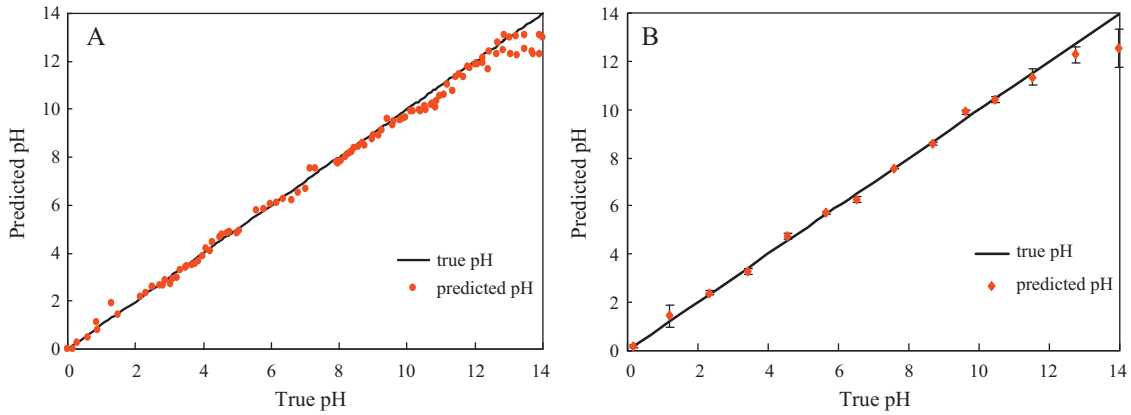

Fig. 10. (A) Comparison between the modelling prediction of the four sensing elements (symbols) and validation experimental data (line) in the full pH range. (B) Comparison between pH values obtained from our system (symbols) and those measured by a reference method (line) for real samples. Error bars show three times the standard deviation of the values obtained with the proposed pH-meter.

H variation of the sensor array in that range as is apparent in Figs. 6 and 7.

The main technical specifications of the developed instrument are listed in Table 4. The resolution was calculated as follows: the coordinates RGB resulting from a colour measurement are coded as a 12-bit word each one. Therefore, the *H* parameter could be expressed as a 12-bit word since it is calculated as a linear combination of RGB coordinates. Assuming a worst case in which only 10 bits are significative and a range of *H* from −0.3 to 1 (Fig. 9), the resolution of *H* is 0.0013. Taking into account that the corresponding pH range is 0–14, the resolution in units of pH is approximately 0.02. The accuracy is obtained from the validation data as the standard deviation. The value from this calculation is 0.2. The response time of the instrument was obtained as the sum of the response of each digital colour sensor which consists of the integration time (200 ms) and the processing of the RGB word (175 ms).

3.2.3. *Application to real samples*

The proposed measurement system was applied to fourteen real water samples (tap and river water from Granada, Spain), with the pH adjusted with acid and base covering the full pH range from 0 to 14. After reaction with samples, the sensor arrays (6 replicates) were measured and the pH values calculated.

The MSE obtained for real water samples was 0.180. As in the case of the validation data set, different tests were applied to check the results. The Kolmogorov–Smirnov test, with a confidence level of 80%, provided the probability values of 0.001 for both test and prediction sets. Since these values are under 0.2, they cannot be assumed to be normal and Student's *t*-test is not reliable. Thus, we applied the Kruskal–Wallis test, with a confidence level of 95%. The probability value obtained was 0.9268 (higher than 0.05), so we can assume that there are no significant differences between the real (found by glass electrode potentiometry) and predicted pH values in the test data set. The Pearson correlation test provided a probability value under 2.07×10^{-14}, showing that there is a significant correlation between the reference and predicted values. The good correlation coefficient R^2 calculated (0.997) ensures a high positive correlation between the real and predicted data (Fig. 10B). These results confirm that the instrument is an efficient tool to automatically measure pH in solutions within a very wide range and with acceptable accuracy.

Table 4
Technical specifications.

Number of sensors	12 max.
pH range	0–14
Resolution	0.02
Accuracy	0.2
Response time	1.5 s
Dimensions	15 cm × 17 cm × 5 cm
Weight	400 g
Connectivity	USB 2.0
Power	PP3 battery

4. Conclusions

A portable optical multianalyte instrument with up to twelve sensing channels is presented and used for the determination of the full pH range. The analytical procedure is based on the colour determination of an array of four sensing membranes. This characteristic produces a very simple electronic design with an important reduction in the number of electronic components. The light source, an OLED programmable display, and an array of digital colour detectors were responsible for colour coordinate determination. A complete analytical and technical characterization was carried out, showing a good agreement with pH measurements from reference instruments. This resulted in a microcontrol-based easy-to-use measurement system with high optical and electrical interference immunity and extremely simple digital signal processing circuitry with commercially available electronic components. The MSE obtained for real water samples was 0.180, which is worse than those obtained in previous work using a Sigmoid competition approach (0.111) or neural networks (0.043), but it can be acceptable for a portable instrument [20,21].

Acknowledgements

We acknowledge financial support from the Ministerio de Ciencia e Innovación, Dirección General de Investigación y Gestión del Plan Nacional de I+D+i (Spain) (Projects CTQ2009-14428-C02-01 and CTQ2009-14428-C02-02); and the Junta de Andalucía (Proyecto de Excelencia P08-FQM-3535). These projects were partially supported by European Regional Development Funds (ERDF).

References

[1] J. Workman, M. Koch, B. Lavine, R. Chrisman, Process Analytical Chemistry, Anal. Chem. 81 (2009) 4623.
[2] W. Gopel, Chemical imaging: I. Concepts and visions for electronic and bioelectronic noses, Sens. Actuators B 52 (1998) 125.
[3] A. Roda, M. Guardigli, P. Pasini, M. Mirasoli, E. Michelini, M. Musiani, Bio- and chemiluminescence imaging in analytical chemistry, Anal. Chim. Acta 541 (2005) 25.
[4] A. Abbaspour, M.A. Mehrgardi, A. Noori, M.A. Kamyabi, A. Khalafi-Nezhad, M.N. Soltani Rad, Speciation of iron(II), iron(III) and full-range pH monitor-

ing using paptode: a simple colorimetric method as an appropriate alternative for optodes, Sens.Actuators B 113 (2006) 857.
[5] A Safavi, N. Maleki, A. Rostamzadeh, S. Maesum, CCD camera full range pH sensor array, Talanta 71 (2007) 498.
[6] B.P. Corgier, C.A. Marquette, L.J. Blum, Screen-printed electrode microarray for electrochemiluminescent measurements, Anal. Chim. Acta 538 (2005) 1.
[7] T.E. Curey, A. Goodey, A. Tsao, J. Lavigne, Y. Sohn, J.T. McDevitt, E.V. Anslyn, D. Neikirk, J.B. Shear, Characterization of multicomponent monosaccharide solutions using an enzyme-based sensor array, Anal. Biochem. 293 (2001) 178.
[8] T. Mayr, G. Liebsch, I. Klimant, O.S. Wolfbeis, Multi-ion imaging using fluorescent sensors in a microtiterplate array format, Analyst 127 (2002) 201.
[9] F.J. Steemers, D.R. Walt, Multi-analyte sensing: from site-selective deposition to randomly-ordered addressable optical fiber sensors, Mikrochim. Acta 131 (1999) 99.
[10] J.J. Lavigne, E.V. Anslyn, Sensing a paradigm shift in the field of molecular recognition: from selective to differential receptors, Angew. Chem. Int. Ed. 40 (2001) 3118.
[11] Y. Vlasov, A. Legin, A. Rudnitskaya, C. Di Natale, A. D'Amico, Nonspecific sensor arrays (electronic tongue) for chemical analysis of liquids: (IUPAC technical report), Pure Appl. Chem. 77 (2005) 1965.
[12] K.L. Michael, L.C. Taylor, S.L. Schultz, F. Szurdoki, D.R. Walt, Making sensors out of disarray: optical sensor microarrays, Proc. SPIE 3270 (1998) 34.
[13] D.R. Walt, Techview: molecular biology. Bead-based fiber-optic arrays, Science 287 (2000) 451.
[14] A.P. Goodey, J.J. Lavigne, S.M. Savoy, M.D. Rodriguez, T. Curey, A. Tsao, G. Simmons, J. Wright, S.J. Yoo, Y. Sohn, E.V. Anslyn, J.B. Shear, D.P. Neikirk, J.T. McDevitt, Development of multianalyte sensor arrays composed of chemically derivatized polymeric microspheres localized in micromachined cavities, J. Am. Chem. Soc. 123 (2001) 2559.
[15] J.J. Lavigne, S. Savoy, M.B. Clevenger, J.E. Ritchie, B. McDoniel, S.J. Yoo, E.V. Anslyn, J.T. McDevitt, J.B. Shear, D. Neikirk, Solution-based analysis of multiple analytes by a sensor array: toward the development of an "electronic tongue", J. Am. Chem. Soc. 120 (1998) 6429.
[16] N.T. Greene, S.L. Morgan, K.D. Shimizu, Molecularly imprinted polymer sensor arrays, Chem. Commun. (2004) 1172.
[17] L. Baldini, A.J. Wilson, J. Hong, A.D. Hamilton, Pattern-based detection of different proteins using an array of fluorescent protein surface receptors, J. Am. Chem. Soc. 126 (2004) 5656.
[18] C. Zhang, K.S. Suslick, A colorimetric sensor array for organics in water, J. Am. Chem. Soc. 127 (2005) 11548.
[19] J. Janata, Do optical sensors really measure pH? Anal. Chem. 59 (1987) 1351.
[20] S. Capel-Cuevas, M.P. Cuellar, I. De Orbé Payá, M.C. Pegalajar, L.F. Capitan-Vallvey, Full-range optical pH sensor based on imaging techniques, Anal. Chim. Acta 681 (2010) 71.
[21] S. Capel-Cuevas, M.P. Cuellar, I. de Orbe-Paya, M.C. Pegalajar, L.F. Capitan-Vallvey, Full-range optical pH sensor array based on neural networks, Microchem. J. 97 (2011) 225.
[22] M.D. Fernandez-Ramos, M. Greluk, A.J. Palma, E. Arroyo-Guerrero, J. Gomez-Sanchez, L.F. Capitan-Vallvey, The use of one-shot sensors with a dedicated portable electronic radiometer for nitrate measurements in aqueous solutions, Meas. Sci. Technol. 19 (2008), 095204/1.
[23] A.J. Palma, A. Lapresta-Fernandez, J.M. Ortigosa-Moreno, M.D. Fernandez-Ramos, M.A. Carvajal, L.F. Capitan-Vallvey, A simplified measurement procedure and portable electronic photometer for disposable sensors based on ionophore-chromoionophore chemistry for potassium determination, Anal. Bioanal. Chem. 386 (2006) 1215.
[24] D. Filippini, S.P.S. Svensson, I. Lundström, Computer screen as a programmable light source for visible absorption characterization of (bio)chemical assays, Chem. Commun. (2003) 240.
[25] S. Macken, C. Di Natale, R. Paolesse, A. D'Amico, I. Lundstroem, D. Filippini, Towards integrated devices for computer screen photo-assisted multi-parameter sensing, Anal. Chim. Acta 632 (2009) 143.
[26] G. Wyszecki, W.S. Stiles, Color Science: Concepts and Methods, Quantitative Data and Formulae, Wiley Classics Library, Denver, USA, 2000.
[27] K. Cantrell, M.M. Erenas, I. Orbe-Paya, L.F. Capitan-Vallvey, Use of the hue parameter of the hue, saturation, value color space as a quantitative analytical parameter for bitonal optical sensors, Anal. Chem. 82 (2010) 531.

Biographies

Antonio Martínez Olmos was born in 1980 in Granada (Spain). He received the MSc degree and the PhD degree in Electronic Engineering from the University of Granada (Granada, Spain) in 2003 and 2009, respectively. Currently he works as Assistant Professor at the University of Granada. His current research includes the design of tomography sensors and the study of optical sensors for different biological measurements.

Sonia Capel Cuevas graduated in chemistry at the University of Granada (Spain) in July 2007. Since 2008 she is a PhD student at the Department of Analytical Chemistry in the University of Granada. Present research interests include the preparation and characterization of colorimetric optical arrays for their use in the analysis of solutions, including them in low-cost portable electronic instruments.

Nuria López Ruiz was born in 1985 in Barcelona (Spain). She received the BS and MSc degree in Telecommunications Engineering in 2003 and 2005, respectively, and the B.S. degree in Electronic Engineering in 2004 from University of Granada (Granada, Spain). Currently she works as research intern at the University of Granada. Her current research interests include the study of different colorimetric and optical sensors and the electronic instrumentation design.

Alberto J. Palma was born in 1968 in Granada (Spain). He received the BS and MSc degrees in physics (Electronics) in 1991 and the PhD degree in 1995 from the University of Granada, Granada, Spain. He is currently an associate professor at the University of Granada. Since 1992, he has been working on trapping of carriers in different electronic devices (diodes and MOS transistors) including characterization and simulation of capture cross sections, random telegraph noise, and generation-recombination noise in devices. From 2000, his current research interest is the study of the application of MOS devices as radiation sensors and the electronic instrumentation design directed to portable, low cost electronic systems in the fields of chemical and physical sensors.

Ignacio de Orbe-Payá is Associate Professor of the Department of Analytical Chemistry at the University of Granada (Spain). His main areas of research are the development of the sensing phases for their use as chemical sensors in the determination of inorganic ions in several matrices; multivariate calibration methods for the quality control of pharmaceutical products and development of analytical methodology using solid-phase spectrometry.

Luis Fermín Capitan-Vallvey, Full Professor of Analytical Chemistry at the University of Granada, received his BSc in Chemistry (1973) and PhD in Chemistry (1986) from the Faculty of Sciences, University of Granada (Spain). In 1983, he founded the Solid Phase Spectrometry group (GSB) and in 2000, together with Prof. Palma López, the interdisciplinary group ECsens, which includes Chemists, Physicists and Electrical and Computer Engineers at the University of Granada. His current research interests are the design, development and fabrication of sensors and portable instrumentation for environmental, health and food analysis and monitoring.